

# The Ring Imaging Cherenkov Detectors of DELPHI.

W. Adam<sup>4</sup>, E. Albrecht<sup>4</sup>, D. Allen<sup>4</sup>, M-L. Andrieux<sup>9</sup>, G. van Apeldoorn<sup>15</sup>, Y. Arnaud<sup>3</sup>, C. Aubret<sup>2</sup>, A. Augustinus<sup>15</sup>, P. Baillon<sup>4</sup>, M. Battaglia<sup>18</sup>, M. Berggren<sup>17</sup>, D. Bloch<sup>6</sup>, O. Botner<sup>19</sup>, C. Bourdarios<sup>10</sup>, J. M. Brunet<sup>2</sup>, A. P. Budziak<sup>11</sup>, A. Buys<sup>4</sup>, P. Carecchio<sup>9</sup>, P. Carrié<sup>4</sup>, P. Cavalli<sup>9</sup>, G. Cerutti<sup>4</sup>, M. Chevy<sup>13</sup>, E. Christophel<sup>6</sup>, E. Dahl-Jensen<sup>14</sup>, G. Damgaard<sup>14</sup>, N. Dimitriou<sup>7</sup>, B. D'Almagne<sup>10</sup>, M. Davenport<sup>4</sup>, J. Dolbeau<sup>2</sup>, M. Dracos<sup>6</sup>, M. Dris<sup>16</sup>, T. Ekelöf<sup>19</sup>, J. P. Engel<sup>6</sup>, D. Fassouliotis<sup>16</sup>, T. A. Filippas<sup>16</sup>, E. Fokitis<sup>16</sup>, F. Fontanelli<sup>8</sup>, A. Fontenille<sup>9</sup>, D. Fraissard<sup>4</sup>, H. Fürstenau<sup>4</sup>, J. Garcia<sup>17</sup>, E. N. Gazis<sup>16</sup>, D. Gillespie<sup>4</sup>, V. Gracco<sup>8</sup>, L. Guglielmi<sup>2</sup>, F. Hahn<sup>20</sup>, S. Haider<sup>15</sup>, A. Hallgren<sup>19</sup>, W. Hao<sup>15</sup>, P. F. Honoré<sup>2</sup>, K. Huet<sup>13</sup>, S. Ilie<sup>4</sup>, P. Ioannou<sup>1</sup>, P. Juillot<sup>6</sup>, E. Karvelas<sup>7</sup>, S. Katsanevas<sup>1</sup>, E. Katsoufis<sup>16</sup>, N. Kjaer<sup>14</sup>, P. M. Kluit<sup>15</sup>, B. Koene<sup>15</sup>, C. Kourkouvelis<sup>1</sup>, G. Lecoœur<sup>4</sup>, G. Lenzen<sup>20</sup>, L-E. Lindqvist<sup>19</sup>, A. López Agüera<sup>17</sup>, D. Loukas<sup>7</sup>, S. Maltezos<sup>16</sup>, A. Markou<sup>7</sup>, J. Medbo<sup>19</sup>, J. Michalowski<sup>11</sup>, F. Montano<sup>8</sup>, G. Mourgue<sup>4</sup>, B. S. Nielsen<sup>14</sup>, R. Nicolaidou<sup>1</sup>, Th. D. Papadopoulou<sup>16</sup>, A. Petrolini<sup>8</sup>, D. Poutot<sup>2</sup>, G. Polok<sup>11</sup>, H. Rahmani<sup>16</sup>, M. Reale<sup>20</sup>, L. K. Resvanis<sup>1</sup>, G. Sajot<sup>9</sup>, M. Sannino<sup>8</sup>, E. Schyns<sup>20</sup>, S. Squarcia<sup>8</sup>, P. Stassi<sup>9</sup>, R. Strub<sup>6</sup>, J. Thadome<sup>20</sup>, G. E. Theodosiou<sup>7†</sup>, M. J. Tobar<sup>4</sup>, D. Z. Toet<sup>15</sup>, L. Trapedini<sup>8</sup>, G. Tripodi<sup>8</sup>, G. Tristram<sup>2</sup>, A. Tsirou<sup>4</sup>, O. Ullaland<sup>4</sup>, A. S. de la Vega<sup>5</sup> and M. Zavrtanik<sup>12</sup>

<sup>1</sup>University of Athens, Physics Department, Physics Laboratory, Solonos Str. 104, GR-10680 Athens, Greece.

<sup>2</sup>Collège de France, Laboratoire de Physique Corpusculaire, 11 place Marcelin-Berthelot, F-75231 Paris, France.

<sup>3</sup>CENS Centre d'Etudes Nucléaires de Saclay, DSM/DAPNIA/SPP, Service de Physique des Particules, F-91191 Gif-sur-Yvette Cedex, France.

<sup>4</sup>CERN, CH-1211 Geneva 23, Switzerland.

<sup>5</sup>COPPE/UF RJ, Dept. de Física, Universidad Federal do Rio de Janeiro, Ilha do Fundão, 21945 Rio de Janeiro, Brazil.

<sup>6</sup>CRN Centre de Recherches Nucléaires, B.P. 20 CRO, F-67037 Strasbourg Cédex, France.

<sup>7</sup>Institute of Nuclear Physics, N.C.S.R. 'Demokritos', P.O. Box 60228, GR-15310 Aghia Paraskevi, Attiki, Greece.

<sup>8</sup>Dipartimento di Fisica, Università di Genova and INFN, Via Dodecaneso 33, I-16146 Genova, Italy.

<sup>9</sup>Institut des Sciences Nucléaires, Université de Grenoble 1, F-38026 Grenoble, France.

<sup>10</sup>LAL Laboratoire de l'Accélérateur Linéaire, Université de Paris-Sud (Paris XI), Bâtiment 200, F-91405 Orsay Cédex, France.

<sup>11</sup>High Energy Physics Laboratory, Inst. of Nucl. Physics, Ul. Kawory 26a, PL-30055 Krakow 30, Poland.

<sup>12</sup>Institut 'Jozef Stefan', Ljubljana, Slovenija.

<sup>13</sup>Université de Mons-Hainaut, Service de Physique des Particules Élémentaires, Faculté des Sciences, Av. Maistriau 15, B-7000 Mons, Belgium.

<sup>14</sup>Niels Bohr Institute, Blegdamsvej 17, DK-2100 Copenhagen, Denmark.

<sup>15</sup>NIKHEF-H, Postbus 41882, NL-1009 DB Amsterdam, The Netherlands.

<sup>16</sup>NTU National Technical University, Physics Laboratory II, 9 Heroes of Polytechnion Street, Zografou, GR-15780 Athens, Greece.

<sup>17</sup>Facultad de Ciencias, Universidad de Santander, av. de los Castros, E-39005 Santander, Spain.

<sup>18</sup>Research Institute for High Energy Physics, SEFT, Siltavuorenpenger 20c, SF-00170 Helsinki, Finland.

<sup>19</sup>Dept. of Radiation Sciences, University of Uppsala, P.O. Box 535, S-751 21 Uppsala, Sweden.

<sup>20</sup>Fachbereich Physik, University of Wuppertal, Gauss-Str. 20, D-42097 Wuppertal, Germany.

†Deceased.

## Abstract

A Ring Imaging Cherenkov (RICH) detector system has been built and is now in full operation within the DELPHI experiment. Large data samples of  $Z^0$  decays are being collected with good resolution on the observed Cherenkov angles. Several studies of  $Z^0$  decays using the RICH have already been performed on limited samples. Disturbance of the detector operation caused by shrinkage of polymeric construction materials and by migration of radiator substance is reported. These effects have been counteracted and do not endanger the quality of the data.

## I. INTRODUCTION

The DELPHI detector at LEP, the Large Electron Positron collider at CERN, is a general purpose particle detector system which is built to give as complete as possible information on each event (fig. 1) [1]. DELPHI is equipped with Ring Imaging Cherenkov (RICH) detectors that provide identification of hadrons. Two RICH systems that are geometrically different but are based on the same operational principles are used. The Barrel RICH is shaped as a cylindrical shell and covers the polar angle range  $40^\circ < \theta < 140^\circ$ . The Forward RICH consists of two endcaps



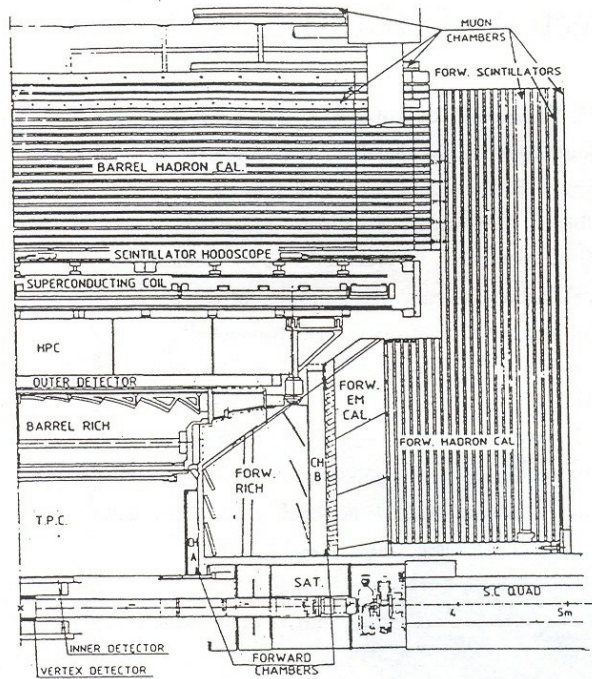


Fig. 1 Cross section of one quadrant of the DELPHI detector. The interaction point is in the lower left corner. The photon detectors of the RICH are found under the labels "RICH".

and covers the two polar angle ranges  $15^\circ < \theta < 35^\circ$  and  $145^\circ < \theta < 165^\circ$ .

The Barrel RICH has been fully installed since 1991 whilst the Forward RICH was completed in 1993. This report deals with recent experience gained through the operation of these large detectors and with some results on their performance.

## II. DETECTOR DESCRIPTION

The RICH detectors have been described in references [2] – [8] and only a brief summary is given here. Both RICH systems combine a liquid and a gaseous radiator to allow particle identification in a wide momentum range. The positions of individual Cherenkov photons are determined in three dimensions by photosensitive Time Projection Chambers (TPC). Precise knowledge of the detector parameters is obtained from a calibration system using UV-light and from a software alignment procedure where  $Z^0 \rightarrow \mu\mu$  events are used. Apart from the detection of Cherenkov photons, identification requires knowledge of the charged particle impact points, directions and momenta. This information is derived from a system of tracking detectors working in the 1.23 T magnetic field of DELPHI.

### A. Cherenkov Radiators

The liquid radiators consist of a 1 cm thick layer of perfluorohexane,  $C_6F_{14}$ , with refractive index 1.28, contained in shallow boxes with quartz windows. These radiators are placed at a distance of about 15 cm in front of the photon detectors and the Cherenkov light produced is projected as a narrow annulus onto the detection plane.

Two different fluorocarbons are used as gaseous radiators, perfluoropentane  $C_5F_{12}$  in the Barrel RICH and perfluorobutane  $C_4F_{10}$  in the Forward RICH, with refractive indices 1.00192 and 1.00150 respectively. The Cherenkov light is projected as ring images onto the detection plane by focusing mirrors [9].

The Barrel RICH is kept at  $40^\circ\text{C}$  since the boiling point of  $C_5F_{12}$  is  $28^\circ\text{C}$ . The boiling point of  $C_4F_{10}$  is  $-2^\circ\text{C}$ . Therefore the Forward RICH is allowed to follow the ambient temperature, which is about  $30^\circ\text{C}$  inside DELPHI. The pressure in the Barrel RICH is stabilized at 1030 hPa, whilst that of the Forward RICH follows the ambient pressure.

### B. Photon Detectors

The photon detectors are segmented TPCs with quartz windows. Each half of the Barrel RICH has 24 TPCs with a drift distance of up to 150 cm. In the Forward RICH the TPCs form truncated sectors spanning  $30^\circ$  in azimuth with Multi Wire Proportional Chambers (MWPCs) along both radial edges. The drift field is established by graded potentials applied to electrodes deposited on the quartz windows and to wires positioned a few cm outside of the drift volumes. The field strength used is 1 kV/cm in the Forward RICH and 0.35 kV/cm in the Barrel RICH. The drift gas fillings are  $C_2H_6$  (Forward RICH) and 75% $CH_4$  + 25% $C_2H_6$  (Barrel RICH) to which has been added  $\sim 0.1\%$  vapor of photoionizable Tetrakis-diMethylAmino-Ethylene (TMAE) molecules. In the Forward RICH the drift direction is perpendicular to the magnetic field, resulting in a Lorentz angle of  $\sim 50^\circ$ . The MWPCs are operated at a gain of  $2 \cdot 10^5$  to allow single electron detection. They have a screening structure limiting the propagation of light from the avalanches at the signal wires.

The TPCs are equipped with a calibration system consisting of a UV flash lamp and optical fibers transmitting the light to an array of known positions in front of the photon detectors. Calibration data are taken continuously during normal physics runs in the Barrel RICH whilst the Forward RICH takes calibration data regularly between these runs. The calibration system provides precise and detailed information about the drift parameters, necessary for the required position resolution [7, 10].



### III. OPERATING EXPERIENCE

The two RICH systems are now in continuous operation with both liquid and gaseous radiators working. A data sample of  $1.5 \cdot 10^6$   $Z^0$  events has been collected in 1994. The earlier  $Z^0$  samples with the Barrel RICH in operation contain about  $4 \cdot 10^5$  events from each of the running periods in 1992 and 1993. The Forward RICH recorded one such sample in 1993.

The operation is generally smooth and data are acquired with high efficiency. Some disturbances have occurred though in the running of these novel detectors and are related to the use of perfluorocarbon radiator substances. Unexpected effects due to purification of the substances with oxygen-removing catalysts have been described earlier, together with the satisfactory results of purification without catalysts [12]. Dimensional changes of polymeric construction materials due to perfluorocarbon exposure and the observation of migration of these substances are reported here, together with the counteractions taken.

#### A. Effects on Construction Materials

The materials used in the construction of the RICH detectors include several polymers. Epoxies are used as glues and in structural components reinforced with fibers of glass, carbon or Kevlar<sup>1</sup>. Epoxy is also employed as a filling material, mixed with glass micro-spheres. Another filling material that has been used is Rohacel<sup>2</sup> foam. The fluid system tubing is mainly made of stainless steel but tubes of the polymers PVC and Rilsan<sup>3</sup> have been used in a few places. Kapton<sup>1</sup> foils cover several surfaces, both to limit outgassing and as a substrate for printed electrodes.

Dimensional changes have been noted on the frames that carry both the electrical field shaping wires and the emitting end of the optical fibers of the UV-light calibration system. These frames are positioned a few cm outside of the Barrel RICH photon detector TPCs. During the data taking period in 1993 occasional corona discharges were observed in one of the TPC sectors. This TPC with its field shaping wire frame was extracted after the data taking and several of the wires on the frame were found slack due to shrinkage of the frame by about 600 ppm. Other frames, inspected inside the Barrel RICH, show similar shrinkage whilst a frame which has never been used in the RICH has not shrunk. It was also found that the voltage degrader bar carrying the resistors that establish the potentials for the TPC and the field shaping wires had shrunk.

A method for reconditioning sectors with shrunk frames has been developed and tested on the extracted sector. The wires are re-tensioned using a spring and more flexible connections are established from the degrader bar to the wire frame and to the TPC drift-volume.

<sup>1</sup>Product of DuPont de Nemours, Geneva.

<sup>2</sup>Product of Röhm, Darmstadt.

<sup>3</sup>Product of Elf Atochem, Paris.

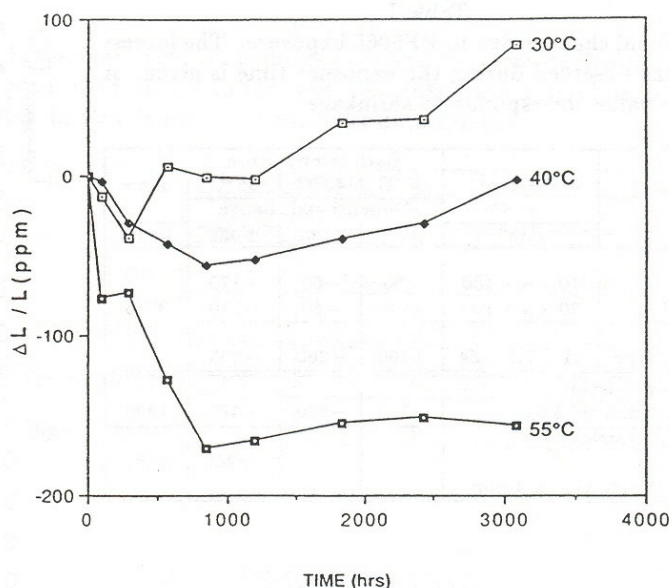


Fig. 2 Modification of length in samples of G-10 plates (with woven glass-fibers) submitted to PF5060 at different temperatures. Sample sizes  $10 \cdot 6 \cdot 100$  mm<sup>3</sup>.

The corona discharges that occurred during the 1993 running could be terminated by shortly ramping down the high voltage, after which it was possible to re-establish the nominal field. For the 1994 data taking the drift voltage has been lowered from 80 kV to 54 kV, after which no corona discharge has occurred. With the reduced electrical field strength of 0.35 kV/cm diffusion does increase but the Cherenkov resolution has been observed not to degrade. A large scale reconditioning of wire frames is therefore not necessary.

During part of the 1993 run the Barrel RICH liquid radiator system leaked due to shrinkage of small PVC plastic tubes on pressostat units. These tubes have now been blocked. The liquid distribution system has also been modified to allow control over each quadrant separately, grouping only six radiator containers together.

#### B. Tests with $C_6F_{14}$ and polymeric materials

Effects of perfluorocarbons on some of the polymeric construction materials used in the RICH have been investigated by immersing samples in PF5060<sup>4</sup> liquid at different temperatures [11]. Samples of the following materials were tested: G-10 plates (glass fiber reinforced epoxy resin, with the fibers arranged as a woven fabric or as a woollen mat), Kapton (polyimide) foil, Rilsan (polyamide 11) tubes and a common epoxy glue<sup>5</sup>.

Fig. 2 shows the dimensional modification of G-10 samples immersed in PF5060 at three different temperatures.

<sup>4</sup>Product of 3M, USA, mainly  $C_6F_{14}$

<sup>5</sup>Ciba-Geigy, Araldite AW106+HU953U



Table I

Dimensional changes due to PF5060 exposure. The largest deviations observed during the exposure time is given. A negative value corresponds to shrinkage.

Material	Size mm <sup>3</sup>	Bath temperature			Time hours
		30°C	40°C	55°C	
		Dimensional change ppm			
G-10 woven type	10 × 4 × 100	+80	-60	-170	3075
	20 × 4 × 100	+110	-50	-110	
G-10 woollen type	21 × 1.5 × 54	+160	-260	-290	
Kapton polyimide foil 0.125 mm thickness		-150	-200	-370	1200
Rilsan polyamide 11 tube Ø <sub>out</sub> = 6 mm, Ø <sub>in</sub> = 4 mm		-	-	-8300	1380

An initial shrinkage phase is seen to be followed by a swelling phase. The relative importance of the swelling and shrinking mechanisms depends on the sample dimensions and on the bath temperature. Table I summarizes the largest dimensional variations observed for the G-10, Kapton and Rilsan samples.

The mechanical strength of the samples were tested by pulling to rupture<sup>6</sup> and found essentially unaltered for the G-10, Kapton and Rilsan samples. The Kapton material became more brittle as the elongation at break was reduced from ~ 38% to ~ 15%. The shearing strength<sup>7</sup> of the tested epoxy glue was found to increase after 1600 hours in PF5060 at 55°C. This increase is attributed to continued polymerization.

Tests were done on two material combinations remaining from the construction of the RICH. The first material sample was a sandwich of Kapton foil, epoxy-fiberglass and Rohacel (polystyrene) foam which showed large deformations reaching about 600 ppm after 800 hours in PF5060 at 55°C. The second material combination was a spare voltage degrader bar. The degrader bars and the wire frames are constructed from a kernel of epoxy<sup>8</sup> loaded with glass micro-spheres surrounded by a skin of Kevlar-fiberglass-epoxy. Their outside is clad with Kapton foil. This construction was chosen as it has a low thermal expansion, similar to that of quartz. The degrader bar was put into PF5060 at 44°C for 22 days after which it was kept in air at 50°C during 140 days. It had then shrunk by about 150 ppm and was still shrinking. Most of the shrinkage occurred with the bar in warm air; only a small fraction of the shrinkage was observed during the initial wet phase.

The results show that the polymeric and composite materials used in the DELPHI RICH can respond with both swelling and shrinkage after exposure to perfluorocarbon

<sup>6</sup> According to DIN 53455

<sup>7</sup> According to ISO 537

<sup>8</sup> Ciba-Geigy 5052

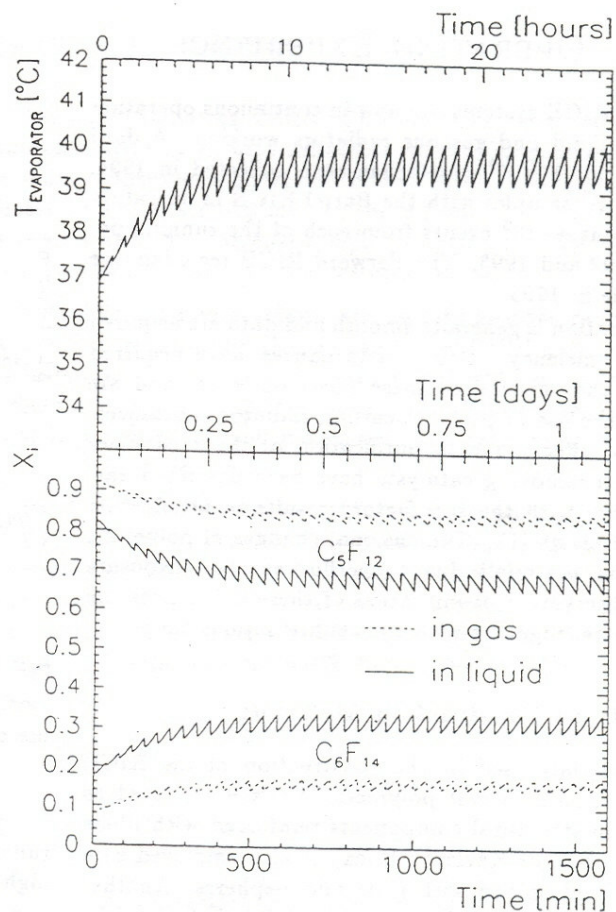


Fig. 3 Calculated time evolution of the temperature in the evaporator (top); and the fractions of  $\text{C}_5\text{F}_{12}$  and  $\text{C}_6\text{F}_{14}$  present in the liquid and the gaseous phase in the evaporator (bottom). An initially empty evaporator and a mixture of 82 %  $\text{C}_5\text{F}_{12}$  with 18 %  $\text{C}_6\text{F}_{14}$  present in the radiator storage tank was assumed. The jagged shape is due to periodic refilling of the evaporator.

liquids. It is therefore likely that the 600 ppm shrinkage that has been observed on the wire frames inside the RICH is indeed due to the exposure to  $\text{C}_5\text{F}_{12}$ . The mechanical strength of the polymers is unaffected though, and with the changed drift voltage the RICH continues to determine photon positions with unaltered resolution, in spite of the occurred shrinkage.

### C. Fluid Migration

The cost of the radiator substances and the need to remove UV-absorbants that are present in the commercially available perfluorocarbons require that these substances are used in a recirculating system with purification. In the gas radiator systems the liquid perfluorocarbon is brought from a storage tank to an evaporator. After passing the RICH vessel the gas is purified and then returns through



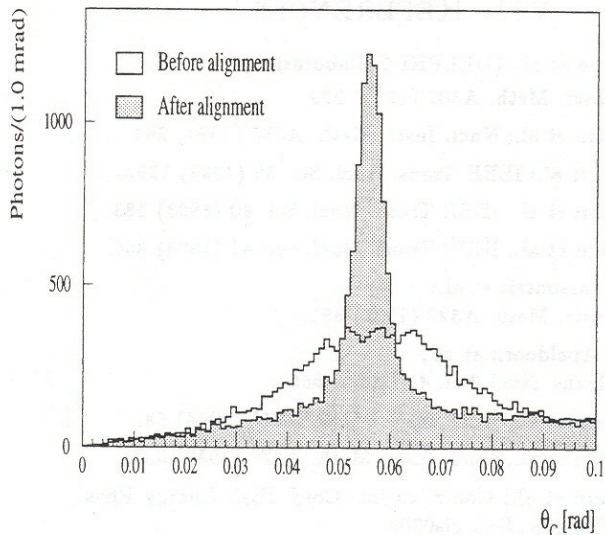


Fig. 4 Distribution of Cherenkov angles from the gas radiator in the Forward RICH for 45 GeV/c muons, before and after alignment.

a liquefier into the storage tank. The systems for the liquid radiators are simpler since neither an evaporator nor a liquefier is needed.

Inside the RICH detectors a migration of perfluorocarbons between the liquid radiator containers and the gas radiator volume occurs, resulting in mixing of the two substances. The substance in the liquid radiator system thus contains an increasing fraction of  $C_5F_{12}$  in the Barrel RICH or  $C_4F_{10}$  in the Forward RICH. Conversely, the gas radiators become contaminated with  $C_6F_{14}$ . Consequently, the evaporator temperature necessary to uphold constant pressure slowly increases. The increase provides a monitor of the mixing ratio of the two perfluorocarbons. An example from calculations of the evaporator temperature and the mixing ratio in the gas and the liquid is shown in fig. 3. The rates of perfluorocarbon migration have in the Barrel RICH been estimated at 0.8 and 1.2 litres/day (liquid volume) for  $C_6F_{14}$  and  $C_5F_{12}$  respectively.

The mixed radiator substances can be separated by distillation. Systems for separation in situ have recently been added to the radiator fluid systems and will limit the minor component to below 10 %. This eliminates the risk of unintended condensation or boiling. Changes of refractive indices will be only marginal and the variation can be followed from the evaporator temperature and from the observed Cherenkov angles. Further, a Fabry-Perot interferometer for determination of refractive indices has been developed and will be installed for the 1995 run.

The migration of radiator substance at the present rate will therefore, with the recent addition of distillation capacity, not reduce the quality of the RICH data.

Table II

Preliminary results on number of photoelectrons detected, photoelectron resolution and Cherenkov angle resolution for 45 GeV/c muons in the 1994 data sample.

	Liquid Radiator		Gas Radiator	
	Photo-electrons	$\sigma$ (mrad)	Photons-electrons	$\sigma$ (mrad)
Barrel RICH	11.7	13.6	8.0	4.6
Cher. Angle		5.2		1.9
Forward RICH	6.8	11.4	6.8	2.7
Cher. Angle		6.1		1.5

## IV. PERFORMANCE

To obtain optimal performance of the RICH system it is important that the refractive indices and the positions of detector components are accurately known. A software alignment package has been developed for this purpose [13, 14]. It uses Cherenkov photons detected in  $e^+e^- \rightarrow Z^0 \rightarrow \mu^+\mu^-$  events where both muons are known to have 45 GeV/c momentum. The UV-light calibration system mentioned in section II provides the detailed input for the photon detector drift properties. The procedure starts from the constructionally known positions of the detector components. A selection of candidate photons is made and the resolution is optimized by varying the positions of radiators, photon detectors and mirrors. The refractive indices of the radiators are varied in the optimization and the observed level of background signals may be accounted for. The importance of the alignment procedure is demonstrated in fig. 4 where the improvement in the resolution is evident.

Dimuon events are further useful to determine the angular resolution of the detector and the amount of Cherenkov light seen. These quantities are summarized in table II. The distributions of observed Cherenkov angles are fitted with a Gaussian distribution superimposed on a background. The single photon resolutions obtained are in good agreement with expectations for the gas radiators whilst they are somewhat worse than calculated for the liquid radiators.

In  $e^+e^- \rightarrow Z^0 \rightarrow q\bar{q}$  events a large number of hadrons, produced in jets, are seen by the detector and result in an increased level of background signals associated to the ring images. However, the detected amount of Cherenkov photoelectrons is sufficient to allow good identification. The identification power is illustrated in fig. 5, where bands corresponding to  $\pi$ , K and p can clearly be seen. Separation of e.g. kaons from pions can be achieved up to  $\sim 20$  GeV/c.



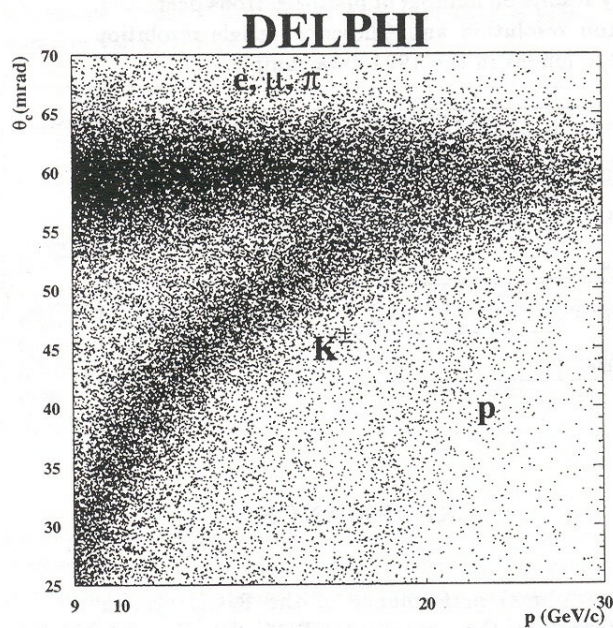


Fig. 5 Cherenkov angles plotted versus particle momenta as observed with the Barrel RICH gas radiator in events with hadron jets.

## V. CONCLUSIONS

The Barrel and Forward RICH detectors of DELPHI are now in full operation utilizing both their liquid and gaseous radiators. The RICH operation has been successfully adapted to the dimensional changes of polymeric materials caused by the perfluorocarbons used, as well as to the migration of these substances between the radiators. After off-line alignment of the detector components a good resolution is obtained for the detected photons. The strong hadron identification power has already been used in published studies of  $Z^0$  decays [15]. Several other studies of  $Z^0$  decays where the information from the RICH is essential are now pursued within DELPHI [16].

## VI. ACKNOWLEDGEMENTS

Many technicians, engineers and physicists from the participating institutes have contributed to the building and commissioning of the RICH detectors. We gratefully acknowledge their devoted efforts, without which the RICH systems could not have become useful in the physics program of DELPHI. Thanks are also due to the many funding agencies that have supported this large project.

## VII. REFERENCES

- [1] P. Aarnio et al.; (DELPHI Collaboration), Nucl. Instr. Meth. A303 (1991) 233.
- [2] W. Adam et al.; Nucl. Instr. Meth. A338 (1994) 284.
- [3] P. Dam et al.; IEEE Trans. Nucl. Sci. 39 (1992) 1292.
- [4] W. Adam et al.; IEEE Trans. Nucl. Sci. 40 (1993) 583.
- [5] W. Adam et al.; IEEE Trans. Nucl. Sci. 41 (1994) 856.
- [6] E.G. Anassontzis et al.; Nucl. Instr. Meth. A323 (1992) 351.
- [7] G. van Apeldoorn et al.; IEEE Trans. Nucl. Sci. 41 (1994) 866.
- [8] W. Adam et al.; Nucl. Instr. Meth. A343 (1994) 68.
- [9] P. Baillon et al.; Nucl. Instr. Meth. A277 (1989) 338.
- [10] W. Adam et al.; Contr. to Int. Conf. High Energy Phys. 1994, Glasgow, Ref. gls0206.
- [11] S. Ilie et al.; Perfluorocarbon effect on composite and polymeric materials used within the DELPHI RICH detectors. DELPHI Internal note, 1994. In preparation.
- [12] S. Ilie, G. Lenzen, Internal note DELPHI 93-33 RICH 54. G. Lenzen et al.; Nucl. Instr. Meth. A343 (1994) 268.
- [13] M. Berggren; ERA - The RICH alignment software package, DELPHI 89-81 PROG 146.
- [14] J. Medbo; DELPHI Internal note, In preparation.
- [15] Published physics analysis reports from the DELPHI collaboration where identification with the RICH has been important.
  - P. Abreu; A measurement of the  $B_s^0$  meson mass, Phys. Lett. B324 (1994) 500.
  - P. Abreu; Charged Kaon Production In Tau Decays at LEP, Phys. Lett. B334 (1994) 435.
- [16] Recent physics analysis conference contributions and internal reports from the DELPHI collaboration where identification with the RICH has been important;
  - Search for exclusive charmless B meson decays with the DELPHI detector at LEP, DELPHI 94-105 PHYS 422, Contributed to ICHEP94, Glasgow, Ref. gls 0163.
  - Measurement of the  $B_d^0$  oscillation frequency using kaons, leptons and jet charge, DELPHI 94-118 PHYS 435; Contributed to ICHEP94, Glasgow, Ref. gls 0171.
  - Production of Charged Particles,  $K_S^0$ ,  $K^\pm$ , p and  $\Lambda$  in  $Z^0 \rightarrow b\bar{b}$  Events and in the Decays of B Hadrons, DELPHI 94-94 PHYS 411, Contributed to ICHEP94, Glasgow, Ref. gls 0181.
  - Search for exclusive decay channels of the  $\Lambda_b^0$  baryon with DELPHI, DELPHI 94-30 PHYS 363.
  - A measurement of the  $\Lambda_c$  baryon production in hadronic  $Z^0$  decays, DELPHI 94-69 PHYS 389.
  - First Measurement of the Strange Quark Asymmetry at the  $Z^0$  Peak, Final draft in preparation, To be submitted to Phys. Lett. B.